Proposed demonstrations of noncontextuality by single particle interferometric analogues of multipartite entanglement

Karl Svozil*

Institut für Theoretische Physik, University of Technology Vienna,

Wiedner Hauptstraße 8-10/136, A-1040 Vienna, Austria

Abstract

The preparation and measurement of the singlet states of two and three two- and three-state particles are enumerated in terms of multiport interferometers for context sensitive configurations. Generalizations to the n particle case are discussed.

PACS numbers: 03.67.Mn,42.50.St

Keywords: Entanglement production, characterization, and manipulation;nonclassical interferometry

*Electronic address: svozil@tuwien.ac.at; URL: http://tph.tuwien.ac.at/~svozil

I. CONTEXTUALITY IN UNIVERSAL QUANTUM NETWORKS

In addition to recent techniques to prepare engineered entangled states in any arbitrary-dimensional Hilbert space [1–4], multiport interferometers could provide feasible quantum channels for physical questions requiring the utilization of higher than two-dimensional states. In what follows, multiport interferometry will be mainly proposed for experimental tests of issues related to proof-of-principle demonstrations of quantum (non)contextuality; in particular to study properties of systems of observables corresponding to interlinked arrangements of tripods in three-dimensional Hilbert space, or interlinked orthogonal bases in higher dimensions.

Contextuality [5–7] has been introduced by Bohr [8] and Bell (Ref. [5], Sec. 5) as the presumption [44] that the *"... result of an observation may reasonably depend not only on the state of the system ... but also on the complete disposition of the apparatus."* That is, the outcome of the measurement of an observable A might depend on which other observables from systems of maximal observables (Ref. [9], p. 173 and Ref. [10], Sec. 84) are measured alongside with A. The simplest such configuration corresponds to an arrangement of five observables A, B, C, D, K with two comeasurable, mutually commuting, systems of operators $\{A, B, C\}$ and $\{A, D, K\}$ called *contexts*, which are interconnected by A. A will be called a *link observable*. This propositional structure can be represented in three-dimensional Hilbert space by two tripods with a single common leg. The multiport interferometers for the preparation of quantum states and detection schemata corresponding to this configuration are enumerated explicitly in Section III.

Proofs of the Kochen-Specker theorem [5, 11–22] utilize properly chosen finite systems of interlinked contexts; every single context corresponding to a system of maximal comeasurable observables. The systems of contexts are chosen for the purpose of showing that there does not exist any consistent possibility to ascribe global truth values by considering all conceivable truth values assignable to the individual contexts—the whole cannot be composed of its parts by adhering to the classical rules, such as the independence of truth values of identical propositions occurring in different parts. One way to consistently maintain interlinked contexts is to give up noncontextuality; i.e., to drop the assertion that the outcome of measurements of (link) observables are independent on the context and are not affected by which other observables are measured concurrently [45]. In that way, contextuality is

introduced as a way to maintain value definiteness for each one of the individual contexts alone.

Indeed, if contextuality is a physically meaningful principle for the finite systems of observables employed in proofs of the Kochen-Specker theorem, then it is interesting to understand why contextuality should not already be detectable in the simplest system of observables $\{A, B, C\}$ and $\{A, D, K\}$ representable by two interlinked tripods as discussed above. Furthermore, in extension of the two-context configuration, also systems of three interlinked contexts such as $\{A, B, C\}$, $\{A, D, K\}$ and $\{K, L, M\}$ interconnected at A and K [46] will be discussed in Section IV.

In what follows, the schema of the proposed experiment will be briefly outlined; for more details, the reader is referred to Refs. [23, 24]. Any unitary operator in finite dimensional Hilbert space can be composed from a succession of two-parameter unitary transformations in two-dimensional subspaces and a multiplication of a single diagonal matrix with elements of modulus 1 in an algorithmic, constructive and tractable manner. The method is similar to Gaussian elimination and facilitates the parameterization of elements of the unitary group in arbitrary dimensions (e.g., Ref. [25], Chapter 2). Reck, Zeilinger, Bernstein and Bertani have suggested to implement these group theoretic results by realizing interferometric analogues of any discrete unitary and hermitean operators in a unified and experimentally feasible way [23, 26]. Early on, one of the goals was to achieve experimentally realizable multiport analogues of multipartite correlation experiments; in particular for particle states in dimensions higher than two. The multiport analogues of many such experiments with higher than two-particle two-dimensional entangled states have been discussed by Zukowski, Zeilinger and Horne [24].

The multiport analogues of multipartite configurations are serial compositions of a preparation and an analyzing multiport interferometer operating with *single* particles at a time. In the preparation phase, a particle enters a multiport interferometer; its wave function undergoing a unitary transformation which generates the state required for a successive measurement. In a second phase, this state is the input of another multiport interferometer which corresponds to the self-adjoint transformation corresponding to the observables. If those observables correspond to multipartite joint measurements, then the output ports represent analogues of joint particle properties. The observables of multiport interferometers are physical properties related to single particles passing through the output ports. Particle

detectors behind such output ports, one detector per output port, register the event of a particle passing through the detector. The observations indicating that the particle has passed through a particular output port are clicks in the detector associated with that port. In such a framework, the spatial locatedness and apartness of the analogous multipartite configuration is not preserved, as single particle events correspond to multipartite measurements. Rather, the emphasis lies on issues such as value definiteness of conceivable physical properties and on contextuality, as discussed above.

There are many forms of suitable two-parameter unitary transformations corresponding to generalized two-dimensional "beam splitters" capable of being the factors of higher than two-dimensional unitary transformations (operating in the respective two-dimensional subspaces). The following considerations are based on the two-dimensional matrix

$$\mathbf{T}(\omega,\phi) = \begin{pmatrix} \sin\omega & \cos\omega \\ e^{-i\phi}\cos\omega & -e^{-i\phi}\sin\omega \end{pmatrix} \tag{1}$$

whose physical realizations in terms of generalized beam splitters are discussed in detail in Appendix A.

In $n > 2$ dimensions, the transformation $\mathbf{T}$ in Eq. (1) can be expanded to operate in two-dimensional subspaces. It is possible to recursively diagonalize any n-dimensional unitary transformation $u(n)$ by a successive applications of matrices of the form of $\mathbf{T}$. The remaining diagonal entries of modulus 1 can be compensated by an inverse diagonal matrix $\mathbf{D}$; such that $u(n)\mathbf{T}'\mathbf{T}''\cdots\mathbf{D} = \mathbb{I}_n$. Thus, the inverse of all these single partial transformations is equivalent to the original transformation; i.e., $u(n) = (\mathbf{T}'\mathbf{T}''\cdots\mathbf{D})^{-1}$. This technique is extensively reviewed in (Ref. [25], Chapter 2), and in [23, 26]. Every single constituent and thus the whole transformation has a interferometric realization.

II. TWO PARTICLES TWO-STATE ANALOGUE

A. States

Let us explicitly enumerate the case of two entangled two-state particles in one of the Bell basis states (e.g., [27]; the superscript T indicates transposition)

$$|\Psi_1\rangle \;=\; \frac{1}{\sqrt{2}}(e_1\otimes e_1 + e_2\otimes e_2) \equiv \frac{1}{\sqrt{2}}(1,0,0,1)^T, \tag{2}$$

$$|\Psi_2\rangle \;=\; \frac{1}{\sqrt{2}}(e_1\otimes e_1 - e_2\otimes e_2) \equiv \frac{1}{\sqrt{2}}(1,0,0,-1)^T, \tag{3}$$

$$|\Psi_3\rangle \;=\; \frac{1}{\sqrt{2}}(e_1\otimes e_2 + e_1\otimes e_2) \equiv \frac{1}{\sqrt{2}}(0,1,1,0)^T, \tag{4}$$

$$|\Psi_4\rangle \;=\; \frac{1}{\sqrt{2}}(e_1\otimes e_2 - e_2\otimes e_1) \equiv \frac{1}{\sqrt{2}}(0,1,-1,0)^T, \tag{5}$$

where $e_1 = (1,0)$ and $e_2 = (0,1)$ form the standard basis of the Hilbert space $\mathbb{C}^2$ of the individual particles. The state operators corresponding to (2)–(4) are the dyadic products of the normalized vectors with themselves; i.e.,

$$|\Psi_1\rangle\langle\Psi_1| \;\equiv\; \frac{1}{2}\begin{pmatrix} 1 & 0 & 0 & 1 \\ 0 & 0 & 0 & 0 \\ 0 & 0 & 0 & 0 \\ 1 & 0 & 0 & 1 \end{pmatrix}, \tag{6}$$

$$|\Psi_2\rangle\langle\Psi_2| \;\equiv\; \frac{1}{2}\begin{pmatrix} 1 & 0 & 0 & -1 \\ 0 & 0 & 0 & 0 \\ 0 & 0 & 0 & 0 \\ -1 & 0 & 0 & 1 \end{pmatrix}, \tag{7}$$

$$|\Psi_3\rangle\langle\Psi_3| \;\equiv\; \frac{1}{2}\begin{pmatrix} 0 & 0 & 0 & 0 \\ 0 & 1 & 1 & 0 \\ 0 & 1 & 1 & 0 \\ 0 & 0 & 0 & 0 \end{pmatrix}, \tag{8}$$

$$|\Psi_4\rangle\langle\Psi_4| \;\equiv\; \frac{1}{2}\begin{pmatrix} 0 & 0 & 0 & 0 \\ 0 & 1 & -1 & 0 \\ 0 & -1 & 1 & 0 \\ 0 & 0 & 0 & 0 \end{pmatrix}. \tag{9}$$

B. Observables

In what follows, we shall consider measurements of states in two-dimensional Hilbert space along four directions spanned by the standard Cartesian basis $\{(1,0),(0,1)\}$ and the basis $\{(1/\sqrt{2})(1,1),(1/\sqrt{2})(-1,1)\}$ obtained by rotating the standard Cartesian basis counterclockwise by the angle $\pi/4$ around the origin. Besides being instructive, this configuration is very useful for further considerations of the generalized three-dimensional cases discussed

in Sections III B and IV.

With the rotation matrix

$$R(\theta) = \begin{pmatrix} \cos\theta & \sin\theta \\ -\sin\theta & \cos\theta \end{pmatrix} \tag{10}$$

two one-particle observables E, F can be defined by

$$E \;=\; \mathrm{diag}(e_{11}, e_{22}), \tag{11}$$

$$F \;=\; R(-\frac{\pi}{4})\; E\; R(\frac{\pi}{4}) = \frac{1}{2}\begin{pmatrix} e_{11}+e_{22} & e_{11}-e_{22} \\ e_{11}-e_{22} & e_{11}+e_{22} \end{pmatrix}. \tag{12}$$

Often, e_{11} and e_{22} are labeled by $0, 1$ or $+, -$, respectively. E and F are able to discriminate between particle states along $\{(1,0),(0,1)\}$ and $\{(1/\sqrt{2})(1,1),(1/\sqrt{2})(-1,1)\}$, respectively.

Let the matrix $[v^T v]$ stand for the the dyadic product of the vector v with itself. Then, E and F could also be interpreted as *context observables,* for each one represents a maximal set of comeasurable observables

$$E \;=\; e_{11}[(1,0)^T\;(1,0)] + e_{22}[(0,1)^T\;(0,1)], \tag{13}$$

$$F \;=\; \frac{e_{11}}{2}\left[(1,1)^T\;(1,1)\right] + \frac{e_{22}}{2}\left[(-1,1)^T\;(-1,1)\right]. \tag{14}$$

In contrast to Sections III and IV, the two contexts are not interlinked; i.e., they do not share a common link observable. The context structure is given by $\{A, B\}$ encoded by the context observable E, and $\{C, D\}$ encoded by the context observable F.

The corresponding single-sided observables for the two-particle case are

$$O_1 \;\equiv\; E \otimes \mathbb{I}_2 \equiv \mathrm{diag}(e_{11}, e_{11}, e_{22}, e_{22}), \tag{15}$$

$$O_2 \;\equiv\; \mathbb{I}_2 \otimes F \equiv \frac{1}{2}\,\mathrm{diag}(F, F) = \frac{1}{2}\begin{pmatrix} e_{11}+e_{22} & e_{11}-e_{22} & 0 & 0 \\ e_{11}-e_{22} & e_{11}+e_{22} & 0 & 0 \\ 0 & 0 & e_{11}+e_{22} & e_{11}-e_{22} \\ 0 & 0 & e_{11}-e_{22} & e_{11}+e_{22} \end{pmatrix}. \tag{16}$$

Here, $\mathrm{diag}(A, B)$ stands for the matrix with diagonal blocks A, B; all other components are zero. $\mathbb{I}_2$ stands for the unit matrix in two dimensions. Thus, for a two-particle setup O_1 measures particle states along $(1,0)$ and $(0,1)$ "on one particle (side)," whereas O_2 measures particle states along $(1/\sqrt{2})(1,1)$ and $(1/\sqrt{2})(-1,1)$ "on the other particle (side)."

As the commutator $[A \otimes \mathbb{I}, \mathbb{I} \otimes B] = (A \otimes \mathbb{I}) \cdot (\mathbb{I} \otimes B) - (\mathbb{I} \otimes B) \cdot (A \otimes \mathbb{I}) \equiv A_{ij}\delta_{lm}\delta_{jk}B_{ms} - \delta_{ij}B_{lm}A_{jk}\delta_{ms} = A_{ik}B_{ls} - B_{ls}A_{ik} = 0$ vanishes for arbitrary matrices A, B, also $[O_1, O_2] = 0$

vanishes, and the two corresponding observables are commeasurable. Hence the two measurements of O_1 and O_2 can be performed successively without disturbing each other.

In order to represent O_1 and O_2 by beam splitters, we note that their eigenvectors form the bases

$$\begin{array}{c} \{(1,0,0,0),(0,1,0,0),(0,0,1,0),(0,0,0,1)\}, \quad \text{and} \\ \{(1/\sqrt{2})(0,0,-1,1),(1/\sqrt{2})(0,0,1,1),(1/\sqrt{2})(-1,1,0,0),(1/\sqrt{2})(1,1,0,0)\} \end{array} \tag{17}$$

with eigenvalues $\{e11, e11, e22, e22\}$ and $\{e22, e11, e22, e11\}$, respectively. By identifying those eigenvectors as rows of a unitary matrix and stacking them in numerical order, one obtains the unitary operators "sorting" the incoming amplitudes into four output ports, corresponding to the eigenvalues of O_1 and O_2, respectively. (Any other arrangement would also do, but would change the port identifications.) That is,

$$U_1 \;=\; \begin{pmatrix} 0 & 0 & 0 & 1 \\ 0 & 0 & 1 & 0 \\ 0 & 1 & 0 & 0 \\ 1 & 0 & 0 & 0 \end{pmatrix}, \tag{18}$$

$$U_2 \;=\; \frac{1}{\sqrt{2}} \begin{pmatrix} 0 & 0 & -1 & 1 \\ 0 & 0 & 1 & 1 \\ -1 & 1 & 0 & 0 \\ 1 & 1 & 0 & 0 \end{pmatrix}. \tag{19}$$

The operator

$$\begin{aligned} O_{12} \;&=\; (E \otimes \mathbb{I}_2) \cdot (\mathbb{I}_2 \otimes F) = E \otimes F \\ &=\; \tfrac{1}{2}\mathrm{diag}(e_{11}F, e_{22}F) = \tfrac{1}{2} \begin{pmatrix} e_{11}(e_{11}+e_{22}) & e_{11}(e_{11}-e_{22}) & 0 & 0 \\ e_{11}(e_{11}-e_{22}) & e_{11}(e_{11}+e_{22}) & 0 & 0 \\ 0 & 0 & e_{22}(e_{11}+e_{22}) & e_{22}(e_{11}-e_{22}) \\ 0 & 0 & e_{22}(e_{11}-e_{22}) & e_{22}(e_{11}+e_{22}) \end{pmatrix} \end{aligned} \tag{20}$$

combines both O_1 and O_2. The interferometric realization of O_{12} in terms of a unitary transformation is the same as for O_2, since they share a common set of eigenstates with different eigenvalues $\{e_{22}^2, e_{11}e_{22}, e_{11}e_{22}, e_{11}^2\}$. Thus, $U_{12} = U_2$.

C. Preparation

The interferometric setup can be decomposed into two phases. In the first phase, the state is prepared. In the second phase, the state is analyzed by successive applications of U_1 and U_2, or just $U_{12} = U_2$, and by observing the output ports.

Suppose the interferometric input and output ports are labeled by $1, \cdots, 4$; and let the corresponding states be represented by $|1\rangle \equiv (1,0,0,0)^T$, $|2\rangle \equiv (0,1,0,0)^T$, $|3\rangle \equiv (0,0,1,0)^T$ and $|4\rangle \equiv (0,0,0,1)^T$. The initial state can be prepared by unitary transformations. For instance, the unitary transformation U_p transforming the state of a particle entering the first port $|1\rangle$ into the singlet state (5) is

$$U_p = \frac{1}{\sqrt{2}} \begin{pmatrix} 0 & -1 & 1 & 0 \\ 1 & 0 & 0 & 1 \\ -1 & 0 & 0 & 1 \\ 0 & 1 & 1 & 0 \end{pmatrix}. \tag{21}$$

D. Predictions

To check the validity of the calculations, consider a measurement of the singlet state $|\Psi_4\rangle$ in (5) with parallel directions. Thus, instead of F in (12), the second operator is the same as E in (11). As a result, $O'_{12} \equiv E \otimes E \equiv \mathrm{diag}(e_1^2, e_1 e_2, e_1 e_2, e_2^2)$. Since the eigenvectors of O'_{12} are just the elements of the standard basis of the Hilbert space $\mathbb{C}^4$, $U'_{12} = U_1$ has only unit entries in its counterdiagonal. Hence, $U'_{12}|\Psi_4\rangle \equiv (1/\sqrt{2})(0,-1,1,0)^T$, and since $|\langle n|U'_{12}|\Psi_4\rangle|^2 = 0$ for $n = 1, 4$ and $|\langle n|U'_{12}|\Psi_4\rangle|^2 = 1/2$ for $n = 2, 3$, there is a 50:50 chance to find the particle in port 2 and 3, respectively. The particle will never be measured in detectors behind the output ports 1 or 4.

These events could be interpreted in the following way: The first and the forth detectors stand for the property that both "single-particle" observables are the same; the second and the third detectors stand for the property that both "single-particle" observables are different. Since the input state was chosen to be a singlet state (5), only the latter case can occur. Similar considerations hold for the other states of the bell basis defined in (2)–(4). In particular, for Ψ_1 and Ψ_2, the detectors behind output ports 1 or 4 will record events, and the detectors behind ports 2 and 3 will not.

The singlet state (5), when processed through U_{12} in Eq. (20), yields equal chances of output through any one of the four output ports of the interferometer; i.e., $U_{12}|\Psi_4\rangle \equiv (1/2)(1,-1,1,1)^T$, and thus $|\langle n|U_{12}|\Psi_4\rangle|^2 = 1/4$, $n = 1,\ldots,4$. This result is consistent with the observation that in (12) the directions of states $\{(1/\sqrt{2})(1,1),(1/\sqrt{2})(-1,1)\}$ measured by F are just the directions of states $\{(1,0),(0,1)\}$ in (11) measured by E rotated counterclockwise by the angle $\pi/4$.

A more general computation for arbitrary $0 \leq \theta \leq \pi$ yields the set

$$\{(\cos\theta,\sin\theta,0,0),(-\sin\theta,\cos\theta,0,0)(0,0,\cos\theta,\sin\theta),(0,0,-\sin\theta,\cos\theta)\}$$

of normalized eigenvectors for $O_{12}(\theta)$. As a result, the corresponding unitary operator is given by

$$U_{12}(\theta) = \mathrm{diag}(R(\theta),R(\theta)) = \begin{pmatrix} \cos\theta & \sin\theta & 0 & 0 \\ -\sin\theta & \cos\theta & 0 & 0 \\ 0 & 0 & \cos\theta & \sin\theta \\ 0 & 0 & -\sin\theta & \cos\theta \end{pmatrix}. \tag{22}$$

Thus, $U_{12}(\theta)|\Psi_4\rangle \equiv (1/\sqrt{2})(\sin\theta,\cos\theta,-\cos\theta,\sin\theta)^T$, and $|\langle 1|U_{12}(\theta)|\Psi_4\rangle|^2 = |\langle 4|U_{12}(\theta)|\Psi_4\rangle|^2 = \frac{1}{2}\sin^2\theta$, $|\langle 2|U_{12}(\theta)|\Psi_4\rangle|^2 = |\langle 3|U_{12}(\theta)|\Psi_4\rangle|^2 = \frac{1}{2}\cos^2\theta$.

E. Interferometric setup

The following sign convention for generalized beam splitters will be used: reflections change the phase by $\pi/2$, contributing a factor $e^{i\pi/2} = i$ to the wave function. Additional phase changes are conveyed by phase shifters. Global phases from mirrors are omitted.

Based on the decomposition of an arbitrary unitary transformation in four dimensions into unitary transformations of two-dimensional subspaces [25], Reck *et al.* [23] have developed an algorithm [28] for the experimental realization of any discrete unitary operator. When applied to the preparation and analyzing stages corresponding to the preparation transformation U_p in Eq. (21) and the analizing transformation U_2 in Eq. (19), respectively, the arrangement is depicted in Fig. 1.

In order to obtain a clearer understanding of the deailed working of the preparation and analizing phases, consider the upper part of Fig. 1 in more detail. This generalized beam splitter represents the preparation transformation U_p enumerated in Eq. (21). Only one

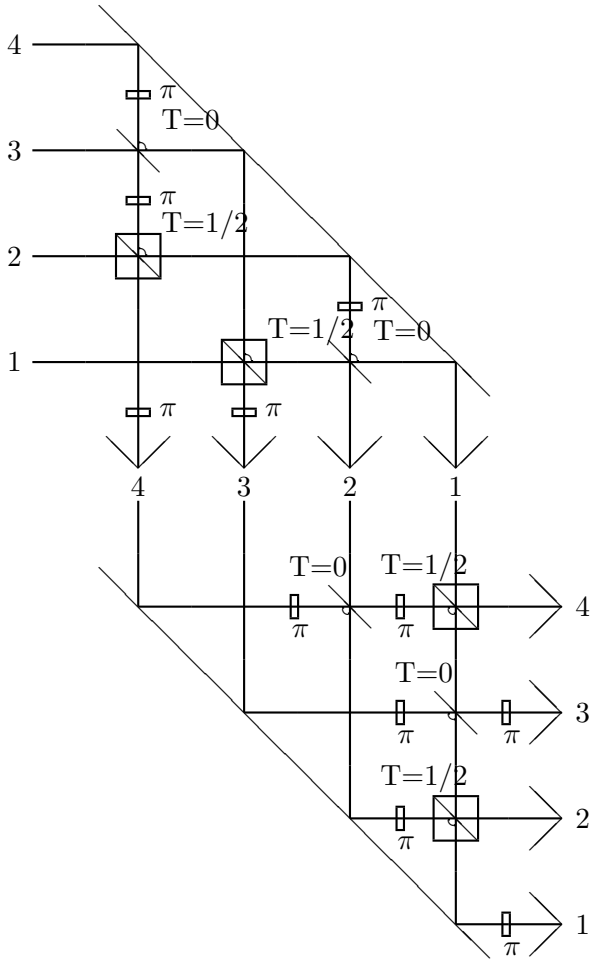

FIG. 1: Preparation and measurement setup of an interferometric analogue of a two two-state particles setup in the singlet state. A single particle enters the upper port number 1 and leaves by one of the lower ports $1, 2, 3$ or 4. Small rectangular boxes indicate phase shifters, big square boxes 50:50 beam splitters ($T = 1/2$), and the $T = 0$ lines depict reflectors.

input port 1 is necessary to obtain the state $|\Psi_4\rangle \equiv \frac{1}{\sqrt{2}}(0, 1, -1, 0)$ defined in Eq. (5) from the state $|1\rangle \equiv (1, 0, 0, 0)^T$. Nevertheless, for the sake of this particular example, the entire pyramid of the complete beam splitter elements corresponding to U_p is depicted. In a later example (cf. Fig. 3), only the bottom part of the pyramid affecting the input port 1 will be drawn. (Even then, not all output ports are required for this particular setup.)

In the upper half of Fig. 1, a particle entering port 1 has a 50:50 chance that it is reflected at or transmitted through the first beam splitter ($T = 1/2$). In the case of reflection, it picks up a phase $\pi/2$, and an additional phase π from the phase shifter in the (intermediate) port

3, collecting an overall phase of $3\pi/2$. In the case of transmission, the particle is reflected ($T = 0$) and leaves by the (intermediate) port 2 with a phase $\pi/2$ from the reflection. (Both intermediate ports 2 and 3 are depicted in the middle of Fig. 1.) Thus the phase difference between the two beam paths 2 and 3 is π, which is responsible for the relative minus sign in $|1\rangle \equiv (1,0,0,0)^T \to |\Psi_4\rangle \equiv \frac{1}{\sqrt{2}}(0,1,-1,0)^T$ (modulo an overall phase of $\pi/2$) for the upper part of Fig. 1.

In a very similar way, the generalized beam splitter in the lower half of Fig. 1 realizes the analizing transformation U_2 in Eq. (19). Thus, the combined effect of the optical elements symbolized in the upper and lower half of Fig. 1 is $|1\rangle \equiv (1,0,0,0)^T \to U_2|\Psi_4\rangle \equiv (1/2)(1,-1,1,1)^T$.

III. TWO PARTICLES THREE-STATE ANALOGUE

A. Singlet state preparation

A group theoretic argument shows that in the case of two three-state particles, there is just one singlet state [29–31]

$$|\Phi\rangle = \frac{1}{\sqrt{3}}(e_1 \otimes e_3 - e_2 \otimes e_2 + e_3 \otimes e_1) \equiv \frac{1}{\sqrt{3}}(0,0,1,0,-1,0,1,0,0)^T, \tag{23}$$

where again $e_1 = (1,0,0)$, $e_2 = (0,1,0)$ and $e_3 = (0,0,1)$ refer to elements of the standard basis of Hilbert space $\mathbb{C}^3$ of the individual particles. A unitary transformation rendering the singlet state (23) from a particle in the first port $|1\rangle$ is

$$U_p = \begin{pmatrix} 0 & 0 & -\frac{1}{\sqrt{3}} & 0 & \frac{1}{\sqrt{3}} & 0 & -\frac{1}{\sqrt{3}} & 0 & 0 \\ 0 & 1 & 0 & 0 & 0 & 0 & 0 & 0 & 0 \\ \frac{1}{\sqrt{3}} & 0 & 0 & 0 & -\frac{1}{\sqrt{3}} & 0 & -\frac{1}{\sqrt{3}} & 0 & 0 \\ 0 & 0 & 0 & 1 & 0 & 0 & 0 & 0 & 0 \\ -\frac{1}{\sqrt{3}} & 0 & -\frac{1}{\sqrt{3}} & 0 & -\frac{1}{\sqrt{3}} & 0 & 0 & 0 & 0 \\ 0 & 0 & 0 & 0 & 0 & 1 & 0 & 0 & 0 \\ \frac{1}{\sqrt{3}} & 0 & -\frac{1}{\sqrt{3}} & 0 & 0 & 0 & \frac{1}{\sqrt{3}} & 0 & 0 \\ 0 & 0 & 0 & 0 & 0 & 0 & 0 & 1 & 0 \\ 0 & 0 & 0 & 0 & 0 & 0 & 0 & 0 & 1 \end{pmatrix}. \tag{24}$$

B. Observables

For the sake of the argument toward quantum (non)contextuality [32], rotations in the $e_1 - e_2$ plane along e_3 are considered; the corresponding matrix being

$$R_{12}(\theta) = \mathrm{diag}(R(\theta), e_{33}) = \begin{pmatrix} \cos\theta & \sin\theta & \\ -\sin\theta & \cos\theta & \\ 0 & 0 & 1 \end{pmatrix} \tag{25}$$

Two one-particle observables E, F can be defined by

$$E \;=\; \mathrm{diag}(e_{11}, e_{22}, e_{33}), \tag{26}$$

$$F \;=\; R_{12}(-\frac{\pi}{4})\; E\; R_{12}(\frac{\pi}{4}) = \frac{1}{2}\begin{pmatrix} e_{11}+e_{22} & e_{11}-e_{22} & \\ e_{11}-e_{22} & e_{11}+e_{22} & \\ 0 & 0 & 2e_{33} \end{pmatrix}. \tag{27}$$

Often, e_{11} and e_{22} are labeled by $-1, 0, 1$, or $-, 0, +$, or $0, 1, 2$, respectively. E and F are able to discriminate between particle states along $\{(1,0,0),(0,1,0),(0,0,1)\}$ and $\{(1/\sqrt{2})(1,1,0),(1/\sqrt{2})(-1,1,0),(0,0,1)\}$, respectively.

E and F could also be interpreted as context observables, for each one represents a maximal set of comeasurable observables

$$E \;=\; e_{11}[(1,0,0)^T\,(1,0,0)] + e_{22}[(0,1,0)^T\,(0,1,0) + e_{33}[(0,0,1)^T\,(0,0,1)], \tag{28}$$

$$F \;=\; \frac{e_{11}}{2}\left[(1,1,0)^T\,(1,1,0)\right] + \frac{e_{22}}{2}\left[(-1,1,0)^T\,(-1,1,0)\right] + e_{33}[(0,0,1)^T\,(0,0,1)]. \tag{29}$$

The two contexts are interlinked at the link observable $A = e_{33}[(0,0,1)^T\,(0,0,1)]$ measuring the particle state along the x_3-axis. The context structure is given by $\{A, B, C\}$ encoded by the context observable E, and $\{A, D, K\}$ encoded by the context observable F.

The corresponding "single-sided" observables for the two-particle case are

$$O_1 \;\equiv\; E \otimes \mathbb{I}_3 \equiv \mathrm{diag}(e_{11}, e_{11}, e_{11}, e_{22}, e_{22}, e_{22}, e_{33}, e_{33}, e_{33}), \tag{30}$$

$$O_2 \;\equiv\; \mathbb{I}_3 \otimes F \equiv \frac{1}{2}\,\mathrm{diag}(F, F, F) = \frac{1}{2}\left(\begin{array}{c|c|c} F & 0 & 0 \\ \hline 0 & F & 0 \\ \hline 0 & 0 & F \end{array}\right). \tag{31}$$

$\mathbb{I}_3$ stands for the unit matrix in three dimensions.

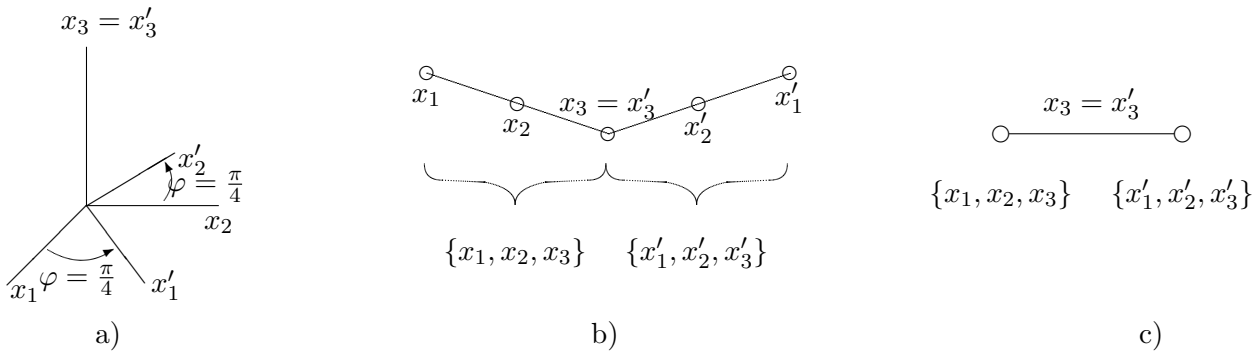

FIG. 2: Three equivalent representation of the same geometric configuration: a) Two tripods with a common leg; b) Greechie (orthogonality) diagram: points stand for individual basis vectors, and orthogonal tripods are drawn as smooth curves; c) Tkadlec diagram: points represent complete tripods and smooth curves represent single legs interconnecting them.

Let $P_1 = [e_1^T e_1] = \mathrm{diag}(1,0,0)$, $P_2 = [e_2^T e_2] = \mathrm{diag}(0,1,0)$, and $P_3 = [e_3^T e_3] = \mathrm{diag}(0,0,1)$ be the projections onto the axes of the standard basis. Then, the following observables can be defined:

$$\begin{aligned} x_1 &= P_1 F = \mathrm{diag}(e_{11}, 0, 0) = B, \\ x_2 &= P_2 F = \mathrm{diag}(0, e_{22}, 0) = C, \\ x_3 &= P_3 F = \mathrm{diag}(0, 0, e_{33}) = A. \end{aligned} \tag{32}$$

Likewise, $x'_1 = D$, $x'_2 = K$ and $x'_3 = A$ can be defined by rotated projections P'_1 and P'_2, and with $P'_3 = P_3$.

The configuration of the observables is depicted in Fig. 2a), together with its representation in a Greechie (orthogonality) diagram [33] in Fig. 2b), which represents orthogonal tripods by points symbolizing individual legs that are connected by smooth curves [47]. In the dual Tkadlec diagram [21] depicted in Fig. 2c), the role of points and smooth curves are interchanged: points represent complete tripods and maximal smooth curves represent single legs. As can already be seen from this simple arrangement of contexts, both Greechie and Tkadlec diagrams are a very compact and useful representation of the context structure; their full power unfolding in proofs of Kochen-Specker theorem [20, 21, 34] requiring a complex structure of multiple interlinked contexts. They are similar to the original diagrammatic representation of Kochen and Specker [15], in which triangles have been used to represent orthogonal tripods and contexts.

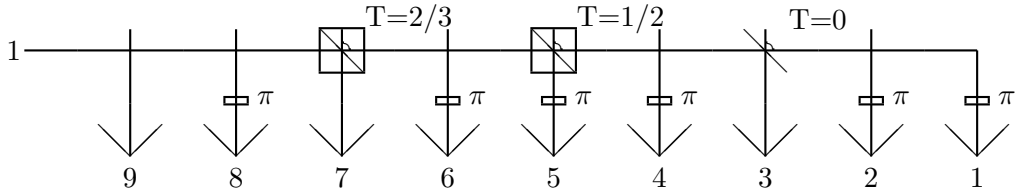

FIG. 3: Preparation stage of a two three-state particles singlet state setup derived from the unitary operator U_p in Eq. (24). Only the bottom part of the element pyramid is drawn.

C. Interferometric implementation

A multiport implementation of U_p in Eq. (24) is depicted in Fig. 3. The entire matrix corresponds to a pyramid of beam splitters and phase shifters, but only the bottom row contributes toward the transformation $|1\rangle \rightarrow |\Phi\rangle$. Note that the phases of the output ports 3,5 and 7 for a particle entering input port 1 is $\pi/2$, $3\pi/2$ and $\pi/2$, respectively. They give rise to the negative sign of the fifth component of $|\Phi\rangle$. The probability that the particle is reflected by the first beam splitter and ends up in port 7 is 1/3. For the remaining particles passing the first beam splitter, there is a 50:50 chance that they end up in ports 3 and 5, respectively; corresponding to the overall probability 1/3 for the activation of these ports. Note that again not all output ports are required for this particular setup. The phase shifters in the output ports 1,2,4,6 and 8 have no particular function for particles entering at port 1, but are necessary to realize the entire transformation U_p in Eq. (24) which requires the complete pyramid of beam splitter elements.

The unitary matrices needed for the interferometric implementation of O_1 and O_2 are again just the ordered eigenvectors of O_1 and O_2; i.e., U_1 is a matrix with unit entries in the

counterdiagonal and zeroes otherwise, and

$$U_2 = \begin{pmatrix} 0 & 0 & 0 & 0 & 0 & 0 & 0 & 0 & 1 \\ 0 & 0 & 0 & 0 & 0 & 0 & -\frac{1}{\sqrt{2}} & \frac{1}{\sqrt{2}} & 0 \\ 0 & 0 & 0 & 0 & 0 & 0 & \frac{1}{\sqrt{2}} & \frac{1}{\sqrt{2}} & 0 \\ 0 & 0 & 0 & 0 & 0 & 1 & 0 & 0 & 0 \\ 0 & 0 & 0 & -\frac{1}{\sqrt{2}} & \frac{1}{\sqrt{2}} & 0 & 0 & 0 & 0 \\ 0 & 0 & 0 & \frac{1}{\sqrt{2}} & \frac{1}{\sqrt{2}} & 0 & 0 & 0 & 0 \\ 0 & 0 & 1 & 0 & 0 & 0 & 0 & 0 & 0 \\ -\frac{1}{\sqrt{2}} & \frac{1}{\sqrt{2}} & 0 & 0 & 0 & 0 & 0 & 0 & 0 \\ \frac{1}{\sqrt{2}} & \frac{1}{\sqrt{2}} & 0 & 0 & 0 & 0 & 0 & 0 & 0 \end{pmatrix}. \tag{33}$$

The interferometric implementation of U_2 is drawn in Fig. 4.

D. Predictions

The probabilities to find the particle in the output ports can be computed by $U_2|\Phi\rangle = (0, -\frac{1}{\sqrt{6}}, \frac{1}{\sqrt{6}}, 0, -\frac{1}{\sqrt{6}}, -\frac{1}{\sqrt{6}}, \frac{1}{\sqrt{3}}, 0, 0)$, and finally $\langle n|U_2|\Phi\rangle$, $n = 1, \ldots, 9$. It is 1/3 for port number 7, 1/6 for ports number 2, 3, 5, 6 and 0 for ports number 1, 4, 8, 9, respectively. This result can be interpreted as follows. Port number 7 corresponds to the occurrence of the observable corresponding to $x_3 \wedge x_3'$, where $\wedge$ stands for the logical *"and."* By convention, the single particle state vectors e_1, e_2, e_3 and their rotated counterparts $e_1', e_2', e_3' = e_3$ can be referred to by the labels "+," "−," "0," respectively; thus port number 7 can be referred to as the "00 case." The ports number 2, 3, 5, 6 correspond to the four equal-weighted possibilities $x_1 \wedge x_1'$, $x_2 \wedge x_2'$, $x_1 \wedge x_2'$, $x_2 \wedge x_1'$, which are also known as $++$, $--$, $+-$, $-+$ cases. The ports number 1, 4, 8, 9 correspond to the four $x_1 \wedge x_3'$, $x_2 \wedge x_3'$, $x_3 \wedge x_1'$, $x_3 \wedge x_2'$, which are also known as $+0$, -0, $0+$, $0-$ cases, which cannot occur, since the particle enters the analyzing part of the interferometer in the singlet state in which it was prepared for.

IV. THREE PARTICLES THREE-STATE ANALOGUE

We shall briefly sketch the considerations yielding to an interferometric realization which is analogous to a configuration of three three-state particles in a singlet state, measured along

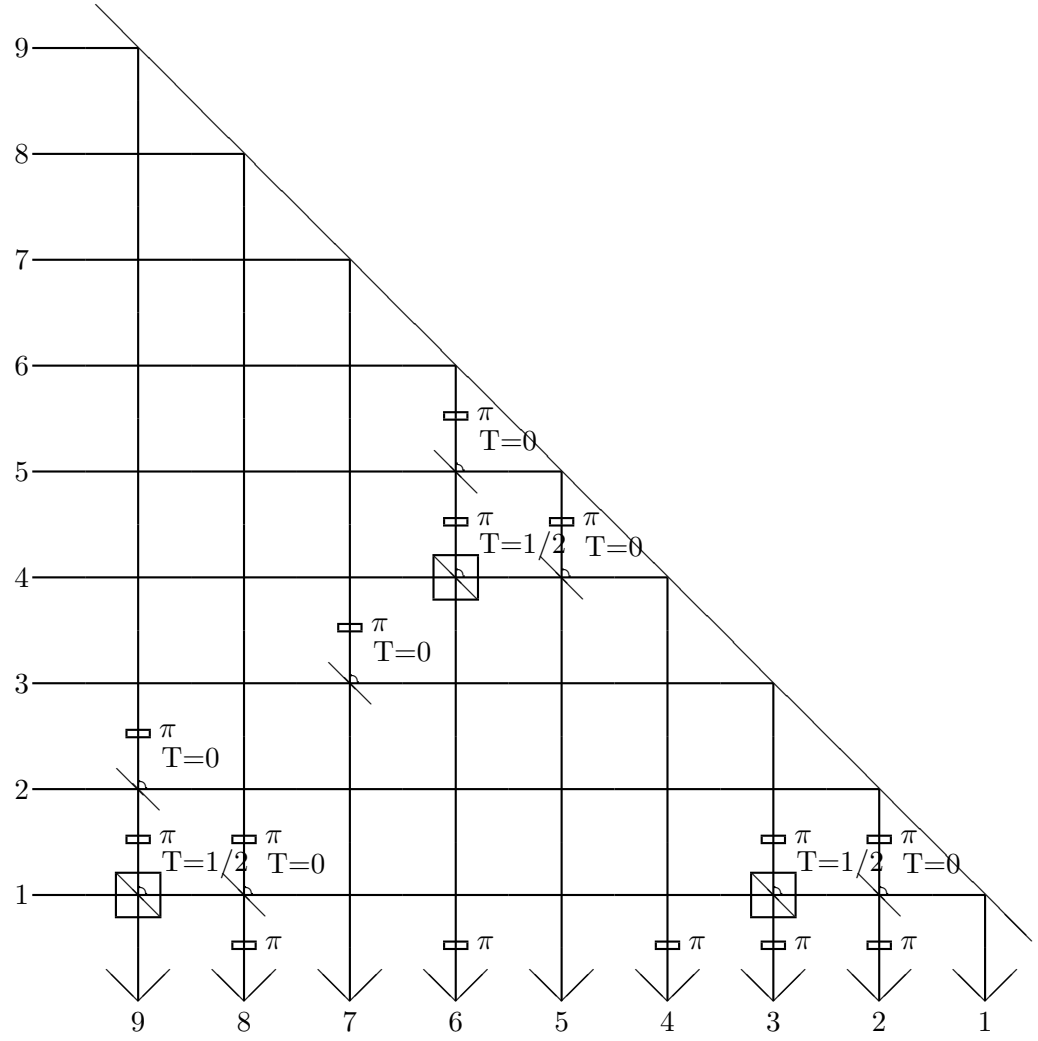

FIG. 4: Measurement setup of an interferometric analogue of a measurement of O_2 in Eq. (33).

three particular directions, such that the context structure is $x_3'' - x_2'' - x_1'' = x_1 - x_2 - x_3 = x_3' - x_1' - x_2'$.

Group theoretic considerations [31, 35] show that the only singlet state for three three-state particles is

$$|\Delta\rangle = \frac{1}{\sqrt{6}}(|-+0\rangle - |-0+\rangle + |+0-\rangle - |+-0\rangle + |0-+\rangle - |0+-\rangle). \tag{34}$$

If the labels "+," "−," "0" are again identified with the single particle state vectors e_1, e_2, e_3 forming a standard basis of $\mathbb{C}^2$, Eq. (34) can be represented by

$$\begin{aligned} |\Delta\rangle &\equiv \tfrac{1}{\sqrt{6}}(e_2\otimes e_1\otimes e_3 - e_2\otimes e_3\otimes e_1 + e_1\otimes e_3\otimes e_2 - e_1\otimes e_2\otimes e_3 + e_3\otimes e_2\otimes e_1 - e_3\otimes e_1\otimes e_2) \\ &\equiv \tfrac{1}{\sqrt{6}}(0,0,0,0,0,-1,0,1,0,0,0,1,0,0,0,-1,0,0,0,-1,0,1,0,0,0,0,0). \end{aligned} \tag{35}$$

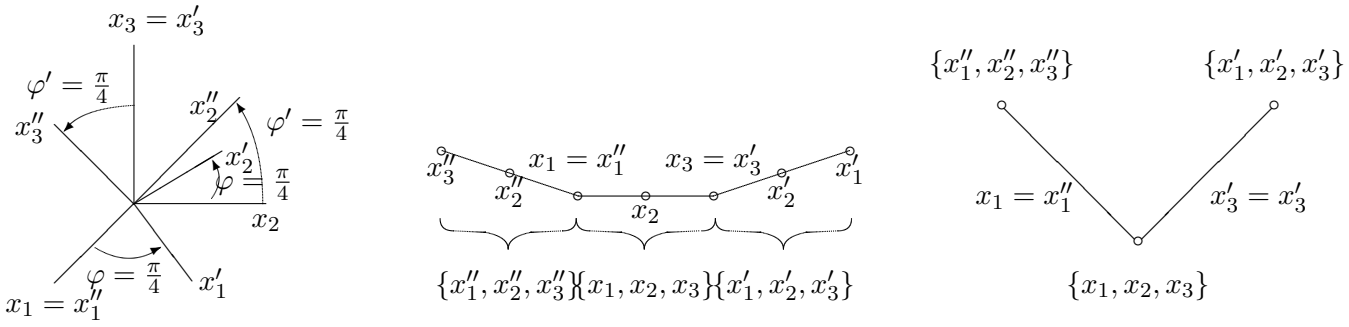

FIG. 5: Three equivalent representation of the same geometric configuration: a) Three tripods interconnected at two common legs; b) Greechie diagram of a); c) Tkadlec diagram of a).

We shall study rotations in the $e_1 - e_2$ plane around e_3, as well as in the in the $e_2 - e_3$ plane around e_1; the corresponding matrix being $R_{23}(\theta) = \mathrm{diag}(e_{11}, R(\theta))$. With the rotation angles $\pi/4$, three one-particle observables E, F, G encoding the contexts $\{A, B, C\}$, $\{A, D, K\}$ and $\{K, L, M\}$, respectively, can be defined by

$$E = \mathrm{diag}(e_{11}, e_{22}, e_{33}), \tag{36}$$

$$F = R_{12}(-\frac{\pi}{4})\ E\ R_{12}(\frac{\pi}{4}), \tag{37}$$

$$G = R_{23}(-\frac{\pi}{4})\ E\ R_{23}(\frac{\pi}{4}). \tag{38}$$

The corresponding single-sided observables for the two-particle case are

$$O_1 \equiv E \otimes \mathbb{I}_3 \otimes \mathbb{I}_3, \tag{39}$$

$$O_2 \equiv \mathbb{I}_3 \otimes F \otimes \mathbb{I}_3, \tag{40}$$

$$O_2 \equiv \mathbb{I}_3 \otimes \mathbb{I}_3 \otimes G. \tag{41}$$

O_1, O_2, O_3 are commeasurable, as they represent analogues of the observables which are measured at the separate particles of the singlet triple. The joint observable

$$O_{123} \equiv E \otimes F \otimes G \tag{42}$$

has normalized eigenvectors which form a unitary basis, whose elements are the rows of the unitary equivalent U_{123} of O_{123}. An interferometric implementation of this operator is depicted in Fig. 6.

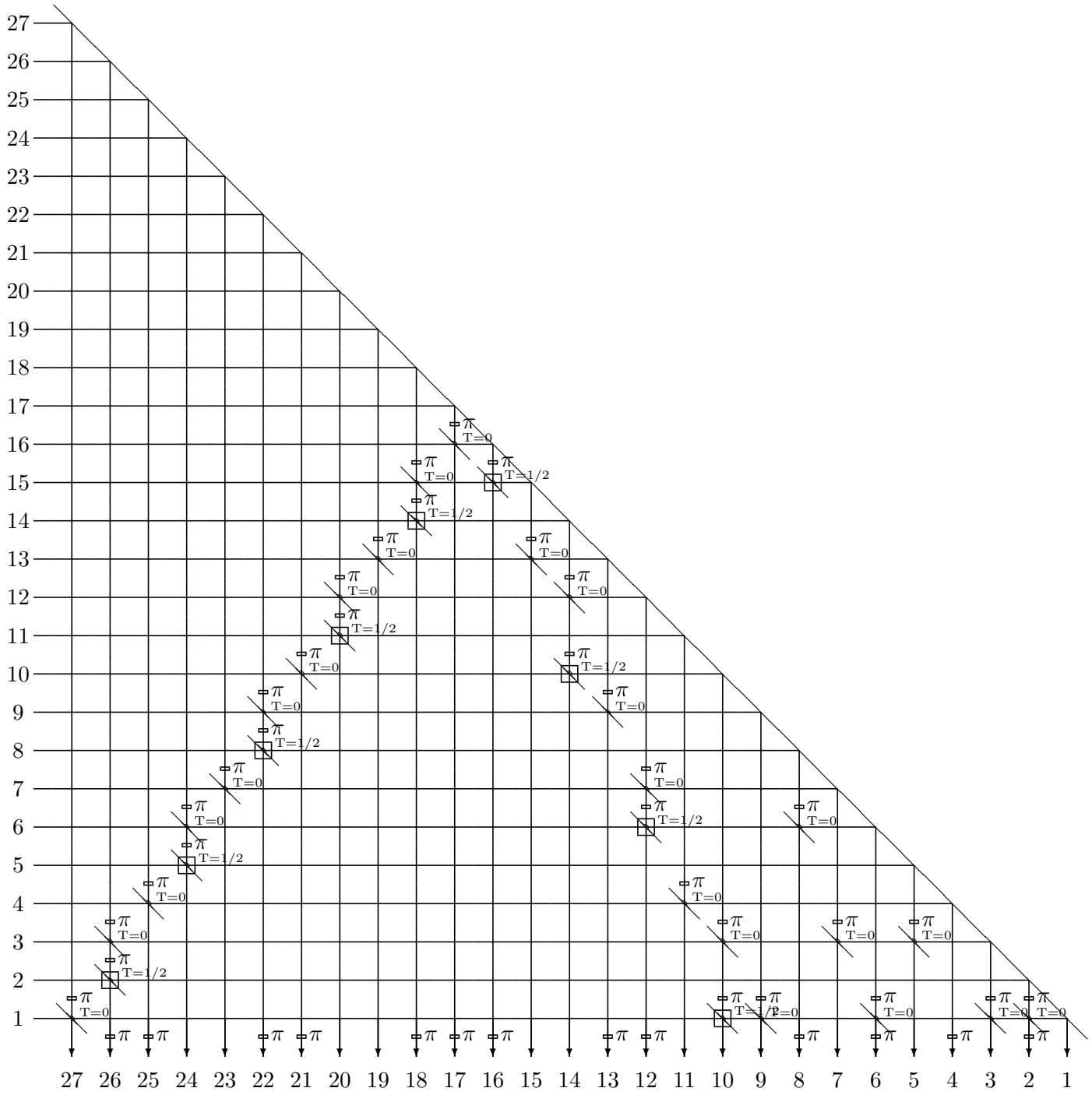

FIG. 6: Measurement setup of an interferometric analogue of a measurement of the three-particle operator O_{123} in Eq. (42).

V. DISCUSSION

Multiport interferometric analogues of multi-particle entanglement have been developed with quantum noncontextuality in mind [32]. Although there is no principal limit to the

number of entangled particles involved, the complexity of the interferometric setup associated with certain tasks, as for example the encoding of "explosion views" of Kochen-Specker configurations, still appears to represent an insurmountable challenge.

Such "explosion views" of Kochen-Specker type configurations of observables can be imagined in the following way. Let N be the number of inter-rotated contexts in the Kochen-Specker type proof. In a first stage, a singlet state of a "large" number N of three-state particles has to be realized. $N = 118$ in the original Kochen-Specker argument [15], and $N = 40$ in Peres' [18, 20] proof. Any such state should be invariant with respect to unitary transformations $u(n^N) = \bigotimes_{i=1}^{N} u_i(n)$ composed of identical unitary transformations $u_i(n)$ in n dimensions. ($n = 3$ in the original Kochen-Specker proof.) Then, every one of the N particle would be measured along the N contexts or blocks, one particle per context, respectively. All steps, in particular the construction and formation of N-partite singlet states by group theoretic methods, as well as the interferometric implementation of these states and of all observables in the many different contexts required by the proof, are constructive and computationally tractable.

These configurations would require an astronomical number (of the order of 3^{80}in the Peres' case of the proof) of beam splitters. Even weaker forms of nonclassicality such as structures with a nonseparating set of states—the Γ_3 in Kochen and Specker's original article [15] would require $N = 16$ (corresponding to sixteen particles) and are still very complex to realize.

There is yet another, principal issue regarding (counterfactually inferred) elements of physical reality. In three dimensions, already three-particle singlet states lack the uniqueness property [32] which in general would allow the unambiguous (counterfactual) inference of three mutually complementary single-particle observables through measurement of the three particles, one observable per particle. Take, for example, $|\Delta\rangle$ in Eq. (34). There are too many coherent orthogonal states contributing to $|\Delta\rangle$ to uniquely fix a single term by the measurement of just one particle. It could be conjectured that, from three particle states onwards, no unique counterfactual reasoning might be possible. Such a property, if it could be proved, would seem to indicate that quantum contextuality cannot be directly measured.

Nevertheless, interferometric analogues of two- and three-particle configurations are realizable with today's techniques. Such configurations have been explicitly enumerated in this article. In experiments realizing singlet states of two particles, no violation of contextuality

can be expected.

For physical implementations, it may be worthwhile to search not only for purely optical implementations of the necessary elementary interferometric cells realizing two-dimensional unitary transformations. Solid state elements and purely electronic devices may be efficient models of multiport interferometric analogues of multipartite entangled states.

Acknowledgments

The kind permission of Michael Reck to use an algorithm for computing and drawing unitary operators as multiport interferometers developed at the University of Innsbruck from 1994-1996 is gratefully acknowledged. Discussions with Peter Kasperkovitz and Stefan Filipp are gratefully acknowledged.

Appendix A: Realizations of two-dimensional beam splitters

In what follows, lossless devices will be considered. The matrix

$$\mathbf{T}(\omega,\phi) = \begin{pmatrix} \sin\omega & \cos\omega \\ e^{-i\phi}\cos\omega & -e^{-i\phi}\sin\omega \end{pmatrix} \tag{A1}$$

introduced in Eq. (1) has physical realizations in terms of beam splitters and Mach-Zehnder interferometers equipped with an appropriate number of phase shifters. Two such realizations are depicted in Fig. 7. The elementary quantum interference device $\mathbf{T}^{bs}$ in Fig. 7a) is a unit consisting of two phase shifters P_1 and P_2 in the input ports, followed by a beam splitter S, which is followed by a phase shifter P_3 in one of the output ports. The device can be quantum mechanically described by [36]

$$\begin{aligned} P_1: \ |\mathbf{0}\rangle &\rightarrow |\mathbf{0}\rangle e^{i(\alpha+\beta)}, \\ P_2: \ |\mathbf{1}\rangle &\rightarrow |\mathbf{1}\rangle e^{i\beta}, \\ S: \ |\mathbf{0}\rangle &\rightarrow \sqrt{T}\,|\mathbf{1}'\rangle + i\sqrt{R}\,|\mathbf{0}'\rangle, \\ S: \ |\mathbf{1}\rangle &\rightarrow \sqrt{T}\,|\mathbf{0}'\rangle + i\sqrt{R}\,|\mathbf{1}'\rangle, \\ P_3: \ |\mathbf{0}'\rangle &\rightarrow |\mathbf{0}'\rangle e^{i\varphi}, \end{aligned} \tag{A2}$$

where every reflection by a beam splitter S contributes a phase $\pi/2$ and thus a factor of $e^{i\pi/2} = i$ to the state evolution. Transmitted beams remain unchanged; i.e., there are no

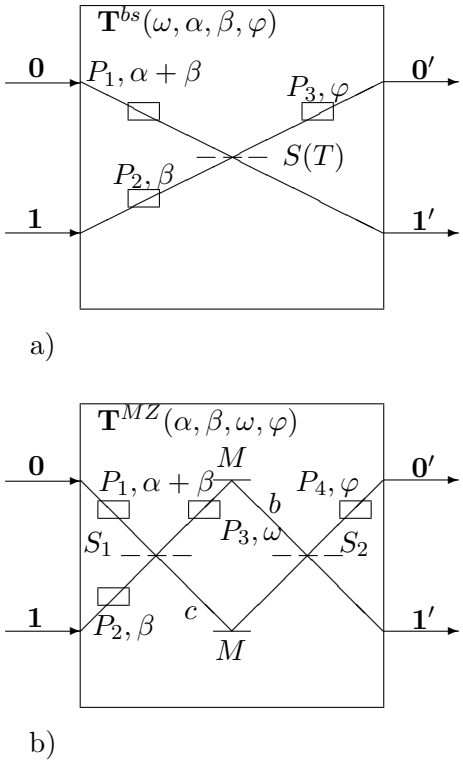

FIG. 7: A universal quantum interference device operating on a qubit can be realized by a 4-port interferometer with two input ports $\mathbf{0}, \mathbf{1}$ and two output ports $\mathbf{0}', \mathbf{1}'$; a) realization by a single beam splitter $S(T)$ with variable transmission T and three phase shifters P_1, P_2, P_3; b) realization by two 50:50 beam splitters S_1 and S_2 and four phase shifters P_1, P_2, P_3, P_4.

phase changes. Global phase shifts from mirror reflections are omitted. With $\sqrt{T(\omega)} = \cos\omega$ and $\sqrt{R(\omega)} = \sin\omega$, the corresponding unitary evolution matrix is given by

$$\mathbf{T}^{bs}(\omega,\alpha,\beta,\varphi) = \begin{pmatrix} i\,e^{i\,(\alpha+\beta+\varphi)}\,\sin\omega & e^{i\,(\beta+\varphi)}\,\cos\omega \\ e^{i\,(\alpha+\beta)}\,\cos\omega & i\,e^{i\,\beta}\,\sin\omega \end{pmatrix}. \tag{A3}$$

Alternatively, the action of a lossless beam splitter may be described by the matrix [48]

$$\begin{pmatrix} i\,\sqrt{R(\omega)} & \sqrt{T(\omega)} \\ \sqrt{T(\omega)} & i\,\sqrt{R(\omega)} \end{pmatrix} = \begin{pmatrix} i\,\sin\omega & \cos\omega \\ \cos\omega & i\,\sin\omega \end{pmatrix}.$$

A phase shifter in two-dimensional Hilbert space is represented by either $\mathrm{diag}\,(e^{i\varphi}, 1)$ or $\mathrm{diag}\,(1, e^{i\varphi})$. The action of the entire device consisting of such elements is calculated by multiplying the matrices in reverse order in which the quanta pass these elements [37, 38];

i.e.,

$$\mathbf{T}^{bs}(\omega,\alpha,\beta,\varphi)=\begin{pmatrix} e^{i\varphi} & 0 \\ 0 & 1 \end{pmatrix}\begin{pmatrix} i\,\sin\omega & \cos\omega \\ \cos\omega & i\,\sin\omega \end{pmatrix}\begin{pmatrix} e^{i(\alpha+\beta)} & 0 \\ 0 & 1 \end{pmatrix}\begin{pmatrix} 1 & 0 \\ 0 & e^{i\beta} \end{pmatrix}. \tag{A4}$$

The elementary quantum interference device $\mathbf{T}^{MZ}$ depicted in Fig. 7b) is a Mach-Zehnder interferometer with *two* input and output ports and three phase shifters. The process can be quantum mechanically described by

$$\begin{aligned} P_1:\ |\mathbf{0}\rangle &\rightarrow |\mathbf{0}\rangle e^{i(\alpha+\beta)}, \\ P_2:\ |\mathbf{1}\rangle &\rightarrow |\mathbf{1}\rangle e^{i\beta}, \\ S_1:\ |\mathbf{1}\rangle &\rightarrow (|b\rangle + i\,|c\rangle)/\sqrt{2}, \\ S_1:\ |\mathbf{0}\rangle &\rightarrow (|c\rangle + i\,|b\rangle)/\sqrt{2}, \\ P_3:\ |b\rangle &\rightarrow |b\rangle e^{i\omega}, \\ S_2:\ |b\rangle &\rightarrow (|\mathbf{1}'\rangle + i\,|\mathbf{0}'\rangle)/\sqrt{2}, \\ S_2:\ |c\rangle &\rightarrow (|\mathbf{0}'\rangle + i\,|\mathbf{1}'\rangle)/\sqrt{2}, \\ P_4:\ |\mathbf{0}'\rangle &\rightarrow |\mathbf{0}'\rangle e^{i\varphi}. \end{aligned} \tag{A5}$$

The corresponding unitary evolution matrix is given by

$$\mathbf{T}^{MZ}(\alpha,\beta,\omega,\varphi)=i\,e^{i(\beta+\frac{\omega}{2})}\begin{pmatrix} -e^{i(\alpha+\varphi)}\sin\frac{\omega}{2} & e^{i\varphi}\cos\frac{\omega}{2} \\ e^{i\alpha}\cos\frac{\omega}{2} & \sin\frac{\omega}{2} \end{pmatrix}. \tag{A6}$$

Alternatively, $\mathbf{T}^{MZ}$ can be computed by matrix multiplication; i.e.,

$$\mathbf{T}^{MZ}(\alpha,\beta,\omega,\varphi)=i\,e^{i(\beta+\frac{\omega}{2})}\begin{pmatrix} e^{i\varphi} & 0 \\ 0 & 1 \end{pmatrix}\frac{1}{\sqrt{2}}\begin{pmatrix} i & 1 \\ 1 & i \end{pmatrix}\begin{pmatrix} e^{i\omega} & 0 \\ 0 & 1 \end{pmatrix}\frac{1}{\sqrt{2}}\begin{pmatrix} i & 1 \\ 1 & i \end{pmatrix}\begin{pmatrix} e^{i(\alpha+\beta)} & 0 \\ 0 & 1 \end{pmatrix}\begin{pmatrix} 1 & 0 \\ 0 & e^{i\beta} \end{pmatrix}. \tag{A7}$$

Both elementary quantum interference devices $\mathbf{T}^{bs}$ and $\mathbf{T}^{MZ}$ are universal in the sense that every unitary quantum evolution operator in two-dimensional Hilbert space can be brought into a one-to-one correspondence with $\mathbf{T}^{bs}$ and $\mathbf{T}^{MZ}$. As the emphasis is on the realization of the elementary beam splitter $\mathbf{T}$ in Eq. (1), which spans a subset of the set of all two-dimensional unitary transformations, the comparison of the parameters in $\mathbf{T}(\omega,\phi) = \mathbf{T}^{bs}(\omega',\beta',\alpha',\varphi') = \mathbf{T}^{MZ}(\omega'',\beta'',\alpha'',\varphi'')$ yields $\omega=\omega'=\omega''/2$, $\beta'=\pi/2-\phi$, $\varphi'=\phi-\pi/2$, $\alpha'=-\pi/2$, $\beta''=\pi/2-\omega-\phi$, $\varphi''=\phi-\pi$, $\alpha''=\pi$, and thus

$$\mathbf{T}(\omega,\phi)=\mathbf{T}^{bs}(\omega,-\frac{\pi}{2},\frac{\pi}{2}-\phi,\phi-\frac{\pi}{2})=\mathbf{T}^{MZ}(2\omega,\pi,\frac{\pi}{2}-\omega-\phi,\phi-\pi). \tag{A8}$$

Let us examine the realization of a few primitive logical "gates" corresponding to (unitary) unary operations on qbits. The "identity" element $\mathbb{I}_2$ is defined by $|\mathbf{0}\rangle \to |\mathbf{0}\rangle$, $|\mathbf{1}\rangle \to |\mathbf{1}\rangle$ and can be realized by

$$\mathbb{I}_2 = \mathbf{T}(\frac{\pi}{2}, \pi) = \mathbf{T}^{bs}(\frac{\pi}{2}, -\frac{\pi}{2}, -\frac{\pi}{2}, \frac{\pi}{2}) = \mathbf{T}^{MZ}(\pi, \pi, -\pi, 0) = \mathrm{diag}\,(1, 1) \quad . \tag{A9}$$

The "not" gate is defined by $|\mathbf{0}\rangle \to |\mathbf{1}\rangle$, $|\mathbf{1}\rangle \to |\mathbf{0}\rangle$ and can be realized by

$$\mathtt{not} = \mathbf{T}(0, 0) = \mathbf{T}^{bs}(0, -\frac{\pi}{2}, \frac{\pi}{2}, -\frac{\pi}{2}) = \mathbf{T}^{MZ}(0, \pi, \frac{\pi}{2}, \pi) = \begin{pmatrix} 0 & 1 \\ 1 & 0 \end{pmatrix} \quad . \tag{A10}$$

The next gate, a modified "$\sqrt{\mathbb{I}_2}$," is a truly quantum mechanical, since it converts a classical bit into a coherent superposition; i.e., $|\mathbf{0}\rangle$ and $|\mathbf{1}\rangle$. $\sqrt{\mathbb{I}_2}$ is defined by $|\mathbf{0}\rangle \to (1/\sqrt{2})(|\mathbf{0}\rangle + |\mathbf{1}\rangle)$, $|\mathbf{1}\rangle \to (1/\sqrt{2})(|\mathbf{0}\rangle - |\mathbf{1}\rangle)$ and can be realized by

$$\sqrt{\mathbb{I}_2} = \mathbf{T}(\frac{\pi}{4}, 0) = \mathbf{T}^{bs}(\frac{\pi}{4}, -\frac{\pi}{2}, \frac{\pi}{2}, -\frac{\pi}{2}) = \mathbf{T}^{MZ}(\frac{\pi}{2}, \pi, \frac{\pi}{4}, -\pi) = \frac{1}{\sqrt{2}} \begin{pmatrix} 1 & 1 \\ 1 & -1 \end{pmatrix} \quad . \tag{A11}$$

Note that $\sqrt{\mathbb{I}_2} \cdot \sqrt{\mathbb{I}_2} = \mathbb{I}_2$. However, the reduced parameterization of $\mathbf{T}(\omega, \phi)$ is insufficient to represent $\sqrt{\mathtt{not}}$, such as

$$\sqrt{\mathtt{not}} = \mathbf{T}^{bs}(\frac{\pi}{4}, -\pi, \frac{3\pi}{4}, -\pi) = \frac{1}{2} \begin{pmatrix} 1+i & 1-i \\ 1-i & 1+i \end{pmatrix}, \tag{A12}$$

with $\sqrt{\mathtt{not}}\sqrt{\mathtt{not}} = \mathtt{not}$.

---

[1] A. Mair, A. Vaziri, G. Weihs, , and A. Zeilinger, Nature **412**, 313 (2001), URL http://dx.doi.org/10.1038/35085529.

[2] A. Vaziri, G. Weihs, , and A. Zeilinger, Physical Review Letters **89**, 240401 (2002), URL http://dx.doi.org/10.1103/PhysRevLett.89.240401.

[3] H. D. Riedmatten, I. Marcikic, H. Zbinden, and N. Gisin, Quantum Information and Computing **2**, 425 (2002), URL http://www.gap-optique.unige.ch/Publications/Pdf/QICfinale.pdf.

[4] J. P. Torres, Y. Deyanova, L. Torner, and G. Molina-Terriza, Physical Review A **67**, 052313 (2003), URL http://dx.doi.org/10.1103/PhysRevA.67.052313.

[5] J. S. Bell, Reviews of Modern Physics **38**, 447 (1966), reprinted in [39, pp. 1-13], URL http://dx.doi.org/10.1103/RevModPhys.38.447.

[6] P. Heywood and M. L. G. Redhead, Foundations of Physics **13**, 481 (1983).

[7] M. Redhead, *Incompleteness, Nonlocality, and Realism: A Prolegomenon to the Philosophy of Quantum Mechanics* (Clarendon Press, Oxford, 1990).

[8] N. Bohr, in *Albert Einstein: Philosopher-Scientist*, edited by P. A. Schilpp (The Library of Living Philosophers, Evanston, Ill., 1949), pp. 200–241, URL http://www.emr.hibu.no/lars/eng/schilpp/Default.html.

[9] J. von Neumann, *Mathematische Grundlagen der Quantenmechanik* (Springer, Berlin, 1932), English translation: *Mathematical Foundations of Quantum Mechanics*, Princeton University Press, Princeton, 1955.

[10] P. R. Halmos, *Finite-dimensional vector spaces* (Springer, New York, Heidelberg, Berlin, 1974).

[11] E. Specker, Dialectica **14**, 175 (1960), reprinted in [40, pp. 175–182]; English translation: *The logic of propositions which are not simultaneously decidable*, reprinted in [41, pp. 135-140].

[12] F. Kamber, Nachr. Akad. Wiss. Göttingen **10**, 103 (1964).

[13] F. Kamber, Mathematische Annalen **158**, 158 (1965).

[14] N. Zierler and M. Schlessinger, Duke Mathematical Journal **32**, 251 (1965).

[15] S. Kochen and E. P. Specker, Journal of Mathematics and Mechanics **17**, 59 (1967), reprinted in [40, pp. 235–263].

[16] V. Alda, Aplik. mate. **25**, 373 (1980).

[17] V. Alda, Aplik. mate. **26**, 57 (1981).

[18] A. Peres, *Quantum Theory: Concepts and Methods* (Kluwer Academic Publishers, Dordrecht, 1993).

[19] N. D. Mermin, Reviews of Modern Physics **65**, 803 (1993), URL http://dx.doi.org/10.1103/RevModPhys.65.803.

[20] K. Svozil and J. Tkadlec, Journal of Mathematical Physics **37**, 5380 (1996), URL http://dx.doi.org/10.1063/1.531710.

[21] J. Tkadlec, International Journal of Theoretical Physics **39**, 921 (2000), URL http://dx.doi.org/10.1023/A:1003695317353.

[22] K. Svozil, *Quantum Logic* (Springer, Singapore, 1998).

[23] M. Reck, A. Zeilinger, H. J. Bernstein, and P. Bertani, Physical Review Letters **73**, 58 (1994), URL http://dx.doi.org/10.1103/PhysRevLett.73.58.

[24] M. Zukowski, A. Zeilinger, and M. A. Horne, Physical Review A **55**, 2564 (1997), URL http://dx.doi.org/10.1103/PhysRevA.55.2564.

[25] F. D. Murnaghan, *The Unitary and Rotation Groups* (Spartan Books, Washington, D.C., 1962).

[26] M. Reck and A. Zeilinger, in *Quantum Interferometry*, edited by F. D. Martini, G. Denardo, and A. Zeilinger (World Scientific, Singapore, 1994), pp. 170–177.

[27] R. Horodecki and M. Horodecki, Physical Review A **54**, 1838 (1996), quant-ph/9607007, URL http://dx.doi.org/10.1103/PhysRevA.54.1838.

[28] M. Reck (1994-1996), mathematica program.

[29] N. D. Mermin, Physical Review D **22**, 356 (1980), URL http://dx.doi.org/10.1103/PhysRevD.22.356.

[30] A. Peres, Physical Review A **46**, 4413 (1992), URL http://dx.doi.org/10.1103/PhysRevA.46.4413.

[31] P. Kok, K. Nemoto, and W. J. Munro (2002), quant-ph/0201138, URL http://arxiv.org/abs/quant-ph/0201138.

[32] K. Svozil (2004), quant-ph/0401112.

[33] J. R. Greechie, Journal of Combinatorial Theory **10**, 119 (1971).

[34] J. Tkadlec, International Journal of Theoretical Physics **37**, 203 (1998), URL http://dx.doi.org/10.1023/A:1026646229896.

[35] P. Kasperkovitz and K. Svozil (2004), in preparation.

[36] D. M. Greenberger, M. A. Horne, and A. Zeilinger, Physics Today **46**, 22 (1993).

[37] B. Yurke, S. L. McCall, and J. R. Klauder, Physical Review A **33**, 4033 (1986), URL http://dx.doi.org/10.1103/PhysRevA.33.4033.

[38] R. A. Campos, B. E. A. Saleh, and M. C. Teich, Physical Review A **42**, 4127 (1990), URL http://dx.doi.org/10.1103/PhysRevA.42.4127.

[39] J. S. Bell, *Speakable and Unspeakable in Quantum Mechanics* (Cambridge University Press, Cambridge, 1987).

[40] E. Specker, *Selecta* (Birkhäuser Verlag, Basel, 1990).

[41] C. A. Hooker, *The Logico-Algebraic Approach to Quantum Mechanics. Volume I: Historical*

Evolution (Reidel, Dordrecht, 1975).

[42] D. A. Meyer, Physical Review Letters **83**, 3751 (1999), quant-ph/9905080, URL `http://dx.doi.org/10.1103/PhysRevLett.83.3751`.

[43] K. Svozil, Journal of Modern Optics **51**, 811 (2004), quant-ph/0308110.

[44] compare Bohr's remarks in Ref. [8] about *"the impossibility of any sharp separation between the behaviour of atomic objects and the interaction with the measuring instruments which serve to define the conditions under which the phenomena appear."*

[45] Other schemata to avoid the Kochen-Specker theorem such as Meyer's [42] restrict the observables such that the construction of inconsistent schemata of interlinked contexts is no more possible. Still other schemata [43] deny the existence of even this restricted set of contexts by maintaining that an n-ary quantum system is only capable of storing exactly one nit of quantum information. Thereby only a single context appears relevant; e.g., the context associated with the particular basis of n-dimensional Hilbert space in which this nit is encoded.

[46] Too tightly interconnected systems such as $\{A, B, C\}$, $\{A, D, K\}$ and $\{K, L, C\}$ have no representation as operators in Hilbert space.

[47] A Greechie diagram consists of *points* which symbolize observables (representable by the spans of vectors in n-dimensional Hilbert space). Any n points belonging to a maximal set of comeasurable observables (representable as some orthonormal basis of n-dimensional Hilbert space) are connected by *smooth curves*. Two smooth curves are crossing in a common link observable. In three dimensions, smooth curves and the associated points stand for tripods.

[48] The standard labeling of the input and output ports are interchanged, therefore sine and cosine are exchanged in the transition matrix.